Progress In Electromagnetics Research C, Vol. 125, 83–92, 2022

A Novel UWB Antenna with Dual Band Notched Characteristics Using a Single Parasitic

Subrahmanyam Grandhi Venkata[1, *] and Sri R. K. Kalva[2]

Abstract—A novel ultrawideband (UWB) antenna with a single parasitic U-type element is reported to exhibit dual-band notch peculiarities. A slotted radiator and a novel defected ground structure (DGS) comprise the proposed antenna, which has a bandwidth of 2.9–11.75 GHz (121%) in the UWB spectrum. By etching a single inverted U-shaped parasitic element on top of the DGS, two rejected bands at the downlink of X-band (6.8–8 GHz) and the uplink of X-band (9.7–11.3 GHz) applications are achieved. The proposed antenna is printed on an FR-4 substrate with a compact size of $24 \times 28\,\text{mm}^2$, has a gain fluctuation of 1.4–5.7 dBi, and a peak radiation efficiency of 92.3%. The suggested antenna is a viable candidate for downlink and uplink X-band notched UWB applications owing to the excellent agreement between its measured and simulated results.

1. INTRODUCTION

The majority of communication systems are intrigued by UWB technology because of its huge impedance bandwidth, simple manufacturing process, low power consumption, increased transmission data speeds, cheap cost, multipath cancellation, and communication security. UWB systems have been customized for employment in the Internet of Things, remote sensing, wearable technology, photography, and broadband cellular satellite communication systems [1]. UWB antennas are crucial in the development of UWB systems. In most applications, the printed monopole antenna (PMA) is the optimal approach since it is simple to construct [2]. Microstrip transmission lines [3] and coplanar waveguide (CPW) [4] are often used in the design of PMAs. In the literature [5, 6], there are many different ways to build planar UWB antennas that can be used in a wide range of practical applications. However, the frequency range from 3.1 to 10.6 GHz includes a variety of licensed narrow band systems, such as WiMAX (3.3–3.6 GHz), 5G (3.4–3.7 GHz), C band (3.7–4.2 GHz), Aeronautical Radio Navigation (ARN) band (4.2–4.7 GHz), WLAN (5.15–5.825 GHz), downlink of X-band satellite communications (7.25–7.75 GHz), and uplink of X-band satellite link (9.6–11.2 GHz). Electromagnetic interference (EMI) is produced by these narrow band systems with UWB systems. The literature [7–11] discusses several approaches for notch single, double, tri, quadruple, and multi-narrow band systems with UWB. To accomplish the 5–5.85 GHz WLAN notched band, an inverted U-type parasitic slit is etched on top of the DGS in [7]. Dual notched bands of 3.3–4 GHz for WiMAX and 5.05–5.90 GHz for WLAN are created by inserting a T-shaped stub in patch and U-shaped parasitic strips beside the feed line [8]. By etching an inverted U-type slot in the patch, a symmetrical split ring resonator pair (SSRRP) proximate to the feed, a C-type parasitic strip on top of DGS, tri-band notched characteristics from 3.78–4.36 GHz for C-band, 5.15–5.45 GHz for lower WLAN, and 7.2–7.9 GHz for X-band downlink are obtained in [9]. The reported antenna is etched with two U-inverted slots in the radiating patch, an SSRRP, and a via hole in [10] to notch four notched bands from 3.25 to 3.55, 3.7 to 4.2, 5.2 to 5.9, and 7 to 7.8 GHz. In [11], four

Received 3 September 2022, Accepted 23 September 2022, Scheduled 6 October 2022

* Corresponding author: Subrahmanyam Grandhi Venkata (subrahmanyam.grandhi@gmail.com).

[1] Department of ECE, Acharya Nagarjuna University College of Engineering and Technology, Guntur, India. [2] Anil Neerukonda Institute of Technology and Sciences, Sangivalasa, Visakhapatnam, India.

rectangular complementary split ring resonators (RCSSRs) on the radiating patch and two RSRRs on the feed line create five rejection bands at 3.5, 4.5, 5.25, 5.7, and 8.2 GHz. In all reported antennas, each band is notched by a different notched element, and hence the UWB system becomes more complex. To reduce UWB system complexity, the proposed antenna notches two X-band rejection bands using a single parasitic element etched on DGS.

This work presents a novel slotted circle-shaped UWB antenna configuration that is loaded with dual band notch features. The intended antenna has a 121% fractional bandwidth throughout an impedance range of 2.9–11.75 GHz. The proposed antenna has a parasitic structure in the shape of an inverted U that notches the 6.8–8 GHz and 9.7–11.3 GHz X-bands for downlink and uplink, respectively. The proposed antenna is good for distortionless wireless UWB applications because it has a peak gain of 5.7 dB, a radiation efficiency of 92.3% in the frequency domain, group delay variations of less than 1 ns, and a minimum isolation of less than −35 dB in the time domain.

2. ANTENNA DESIGN

Figure 1(a) shows the proposed antenna geometry, which uses a single parasitic element to create two notched bands, and Figure 1(b) shows the prototype.

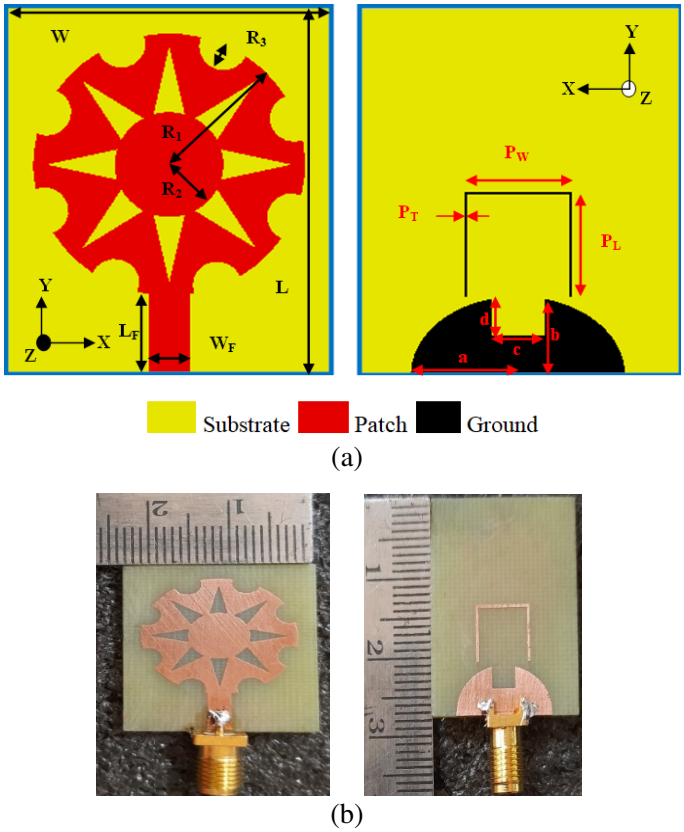

Figure 1. Proposed antenna. (a) Geometry. (b) Prototype.

The proposed antenna is driven through a microstrip line of dimensions ($W_F \times L_F$) and is coated on top of an FR-4 substrate $W \times L$ with a thickness of 1.6 mm. On the back of the substrate, a slotted and modified elliptical ground of major and minor radii 'a' and 'b' is etched in order to increase the bandwidth of the intended antenna. An inverted U-shaped parasitic element with the dimensions $P_W \times P_L \times P_T$ is etched on top of the DGS to reduce the EMI caused by X-band downlink and uplink. The optimized dimensions of the proposed antenna are depicted in Table 1.

Table 1. Optimized dimensions of proposed antenna.

Parameter	Dimension (mm)	Parameter	Dimension (mm)
W	24	a	8
L	28	b	6
W_F	3	c	4
L_F	6.5	d	2.8
P_W	8	R_1	10
P_L	7.7	R_2	4
P_T	0.3	R_3	1.8

3. PARAMETRIC STUDY OF PROPOSED ANTENNA

The successive stages of development of the proposed antenna using parametric investigation are described in this section. The antenna's parametric investigation starts with changing the parameters of the circularly slotted patch, then the defective ground structure, and lastly, the inverted U-shaped parasitic element.

3.1. Parametric Study by Varying Patch Structure

The parametric investigation of the proposed antenna is carried out in five stages by altering the structure of the patch with the proposed DGS, as illustrated in Figures 2(a)–(e), and the S_{11} plot is presented in Figure 3. As shown in Figure 2(a), the Ant#a antenna structure is achieved by joining a circular patch of radius (R_1) to a 50 Ω microstrip line feed, which covers an impedance bandwidth of 3.15–12.9 GHz with peak values of S_{11} of −20.9, −27.2, and −29.7 dB at three resonant frequencies of 3.77, 8.88, and 11.64 GHz, as shown in Figure 3. The antenna structure, Ant#b, shown in Figure 2(b), is developed by etching a four-segment ellipse having major and minor radii of 9 mm and 2 mm from the antenna structure Ant#a and then transforming the slotted structure by thrice at an angle of 45°. As shown in Figure 3, the Ant#b antenna configuration provides three resonant bands operating across 2.9–3.94 GHz with a peak S_{11} of −24.35 at 3.34 GHz, 6.25–7.78 GHz with a peak S_{11} of −15.76 dB at 7.08 GHz, and 9.6–14.54 GHz with a peak S_{11} of −44.89 dB at 11.2 GHz. According to Figure 2(c), Ant#c is obtained by inserting a cylinder with an inner circular radius (R_2) inside the Ant#b antenna configuration. Antenna Ant#c, shown in Figure 3, has two resonant bands that span from 2.99 to 9.76 GHz and have peak S_{11} values of −37.3 dB at 3.47 GHz, −45 dB at 6.28 GHz, −17.3 dB at 9.17 GHz, and 11.4 to 11.8 GHz, with a maximum S_{11} value of −16.2 dB at 11.63 GHz. A circular cylinder of radius (R_3) is notched at the perimeter of the circular patch of radius (R_1) to create the antenna configuration, Ant#d, depicted in Figure 2(d). The antenna geometry, Ant#d, as shown in Figure 3, has three resonant frequencies of 3.75, 8.71, and 11.49 GHz with peak S_{11} values of −21.3, −39.3, and −26.05 dB. The notched structure of Ant#d as shown in Figure 2(d) is transformed by 45° to obtain the proposed patch antenna structure, Ant#e, as depicted in Figure 2(e). As shown in Figure 3, the

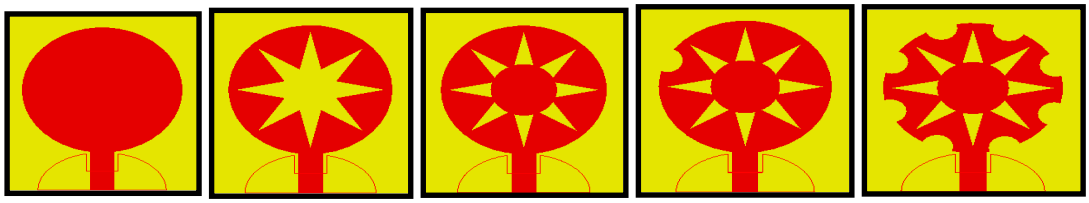

(a) Ant #a (b) Ant #b (c) Ant #c (d) Ant #d (e) Ant #e

Figure 2. Proposed antenna with varying patch structure.

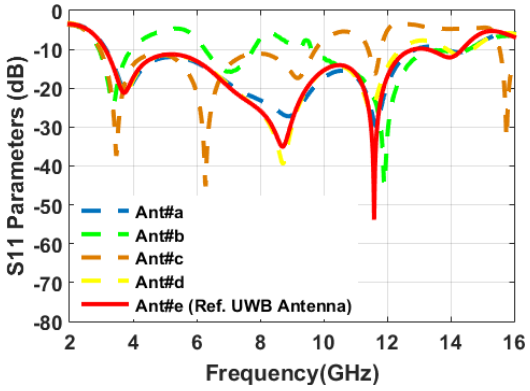

Figure 3. S_{11} plot with varying patch structure.

proposed antenna structure, Ant#e, when being integrated with the proposed DGS, could generate a UWB with a fractional bandwidth of 129% and peak values of S_{11} of -21.1, -34.8, -53.6, and -12.1 dB at four resonant frequencies of 3.72, 8.74, 11.59, and 13.95 GHz.

3.2. Parametric Study by Varying DGS Structure

The proposed antenna's parametric investigation is carried out in four stages by changing the structure of the DGS with the proposed patch structure, as shown in Figures 4(a)–(d), and the S_{11} plot is shown in Figure 5. Initially, the antenna design Ant#1 is formed by notching the whole ground plane with a rectangular DGS that has a size of $(24 \times 6\,\text{mm}^2)$ as shown in Figure 4(a). As shown in Figure 5, the

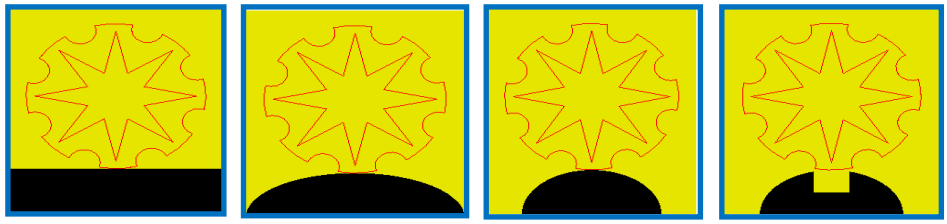

(a) Ant #1 (b) Ant #2 (c) Ant #3 (d) Ant #4

Figure 4. Proposed antenna with varying ground structure.

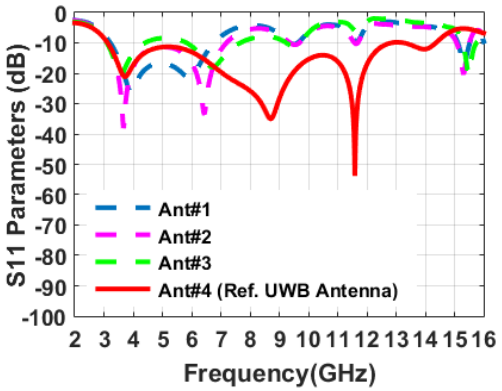

Figure 5. S_{11} plot with varying ground structure.

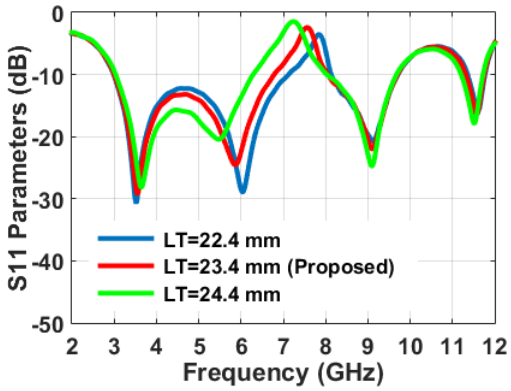

Figure 6. S_{11} plot for different lengths of S-shaped slot for rejection of WLAN band.

antenna denoted as Ant#1 is capable of providing a bandwidth ranging from 3.26 to 6.78 GHz with a peak S_{11} of −26.2 dB at 3.94 GHz and −21.45 dB at 5.93 GHz. The rectangular DGS is modified by an elliptical structure with major and minor radii of 12 and 6 mm as shown in Figure 4(b) to obtain the antenna structures Ant#2, which can provide impedance bandwidth from 3.12 to 7.22 GHz with a peak S_{11} of −37.5 dB at 3.69 GHz and −32.45 dB at 6.46 GHz as shown in Figure 5. By etching an ellipse of 8 and 6 mm as shown in Figure 4(c), Ant#3 can produce three resonant bands across 3.08–4.39, 5.84–7.68, and 9.23–9.74 GHz with S_{11} values of −20.38, −18.02, and −11.15 dB at 3.59, 6.72, and 9.52 GHz, respectively. Finally, Ant#4 is developed by etching a rectangular slot in Ant#3's DGS structure, which can give a −10 dB bandwidth from 3.1 to 14.4 GHz with peak S_{11} values of −21.1, −34.8, −53.6, and −12.1 dB at four resonant frequencies of 3.72, 8.74, 11.59, and 13.95 GHz, as shown in Figure 5.

3.3. Parametric Study for Notched Bands

To stop X-band down/uplink, a single inverted U-shaped parasitic is introduced on top of the DGS. The total length, L_T, of inverted U-type parasitic element is approximated as a half wave length resonator to notch downlink and uplink of X-band as discussed in [12]. When the parasitic length $L_T = P_W + 2P_L$ is 22.4 mm, the notched bands of the proposed antenna are achieved in the frequency ranges of 7.12–8.13 GHz for downlink of X-band and 9.69–11.36 GHz for uplink of X-band. For the proposed parasitic length of L_T = 23.4 mm (Proposed), the two rejection bands of proposed antenna are spanned in between 6.78–8.05 GHz for downlink and 9.68–11.29 GHz for uplink of X-band. When parasitic length is L_T = 24.4 mm, the two rejection bands are obtained at 6.29–8.02 GHz for downlink and 9.67–11 GHz for uplink of X-band as shown in Figure 6.

4. PROPOSED ESA RESULTS AND DISCUSSION

4.1. Frequency Domain Analysis

The designed antenna is simulated by CST ver. 2021 and calibrated by Anritsu MS2037C/2. The calibrated and simulated S_{11} and VSWR plots of proposed antenna are elucidated in Figures 7(a) and (b). There is a little disparity between the calibrated and simulated outcomes of S_{11} and VSWR [13], which can be due to the quality of the SMA connector, measurement errors, and the uncertainty in the value of the dielectric constant (ε_r). According to Figures 7(a) and (b), the proposed antenna's bandwidth ranges from 2.9 to 11.75 GHz. The centre frequencies of two notched bands are 7.56 GHz and 10.54 GHz, respectively, with VSWR values of 7.17 and 3.21, and bandwidths of 1200 MHz and 1600 MHz for notch down/uplink of X-band applications. Figure 8(a) shows the plot of measured peak

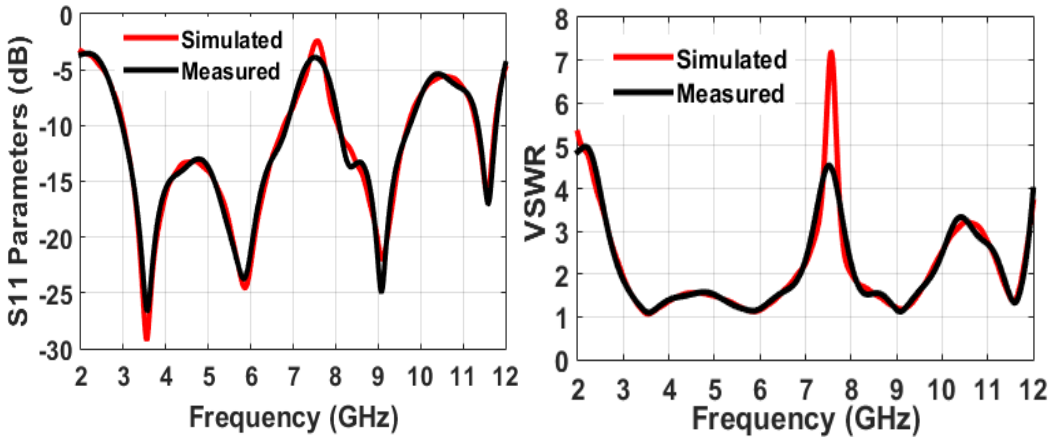

Figure 7. Measured and Simulated S_{11} and VSWR plot of proposed antenna.

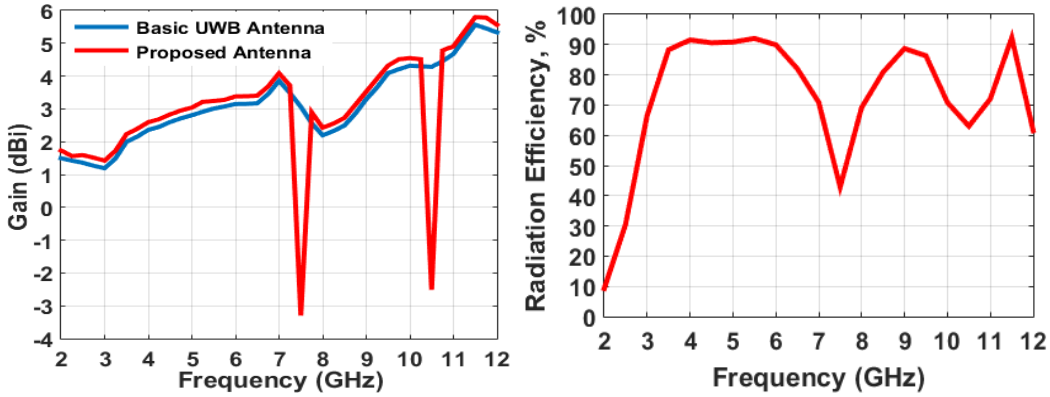

(a) (b)

Figure 8. Peak gain and Radiation efficiency of proposed antenna.

gain vs frequency of the proposed antenna. The peak gain in the operating bandwidth varies from 1.4 to 5.7 dBi, except at the band rejection frequencies of the downlink of X-band (6.8–8 GHz) and the uplink of X-band (9.7–11.3 GHz). Peak gain is measured to be −3.89 dBi and −3.11 dBi for downlink and uplink of X-band notch centre frequencies of 7.56 GHz and 10.54 GHz, respectively. Figure 8(b) shows that the proposed antenna's maximum measured radiation efficiency is 92.32% at 11.5 GHz and drastically decreases to 42.9% and 63.0%, respectively, at the notch centre frequencies of 7.56 GHz and 10.54 GHz.

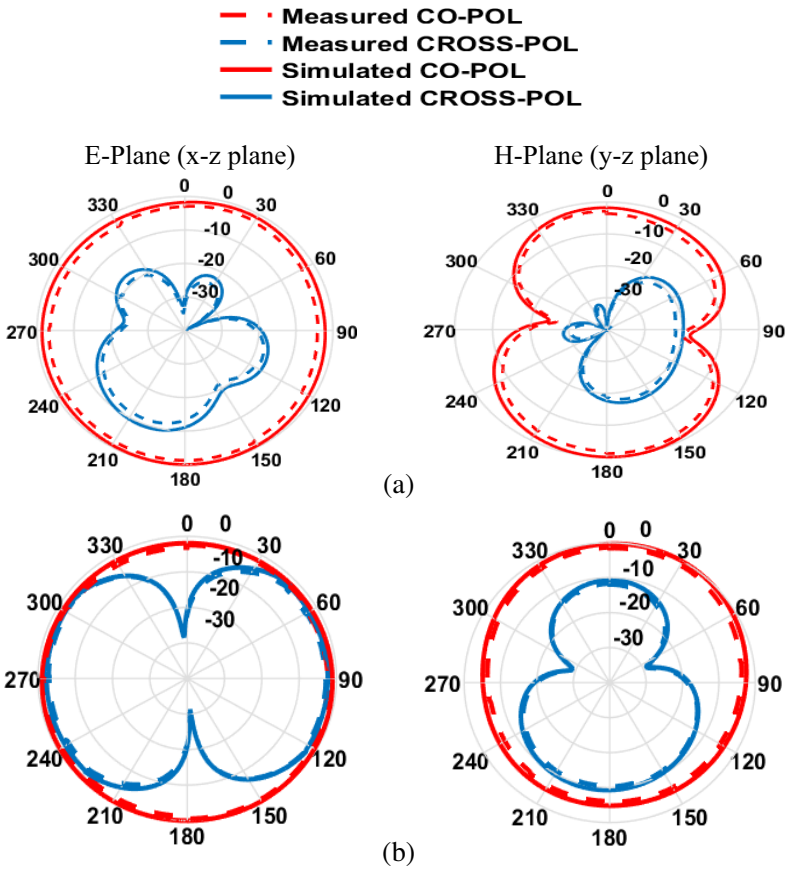

(a)

(b)

Figure 9. Radiation patterns in E- and H-plane. (a) 3.56 GHz, (b) 9.10 GHz.

Figure 9 shows the measured and modeled radiation patterns of the proposed antenna in the E and H planes at two resonant frequencies: 3.56 GHz and 9.10 GHz. At higher frequencies, 9.10 GHz, higher order modes and inconsistent phase distribution on the antenna aperture distort the radiation pattern [14]. The radiation patterns were found to be nearly stable, omnidirectional in the H-plane, and dumbbell shaped in the E-plane.

Figures 10(a), (b), and (d) show the surface current distributions of the proposed antenna at three resonant frequencies of 3.56, 5.86, and 9.10 GHz, while Figures 10(c) and (e) show the surface currents at two notch frequencies of 7.56 GHz and 10.54 GHz. At notched frequencies of 7.56 GHz and 10.54 GHz, the distribution of currents is high around an inverted U-shaped parasitic approach with red areas for the notch of X-band downlink and uplink applications. As a result, the energy is not emitted into the air at these notched frequencies [15]. This mechanism clearly indicates that the proposed antenna effectively eliminates the two bands centred at 7.56 GHz and 10.54 GHz.

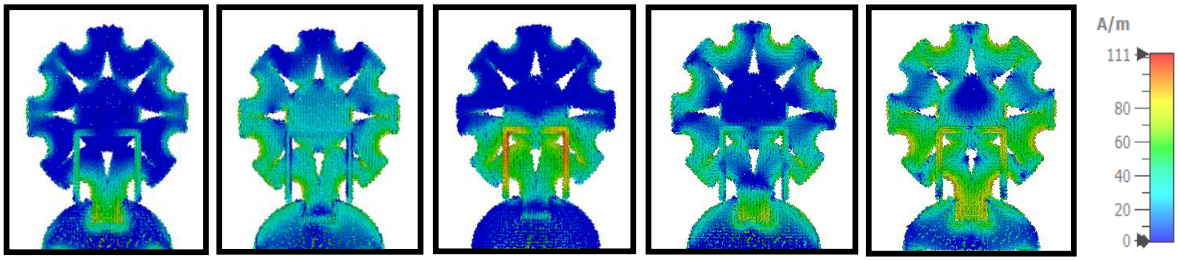

Figure 10. Surface current distributions at (a) 3.56 GHz, (b) 5.86 GHz, (c) 7.56 GHz, (d) 9.1 GHz, (e) 10.54 GHz.

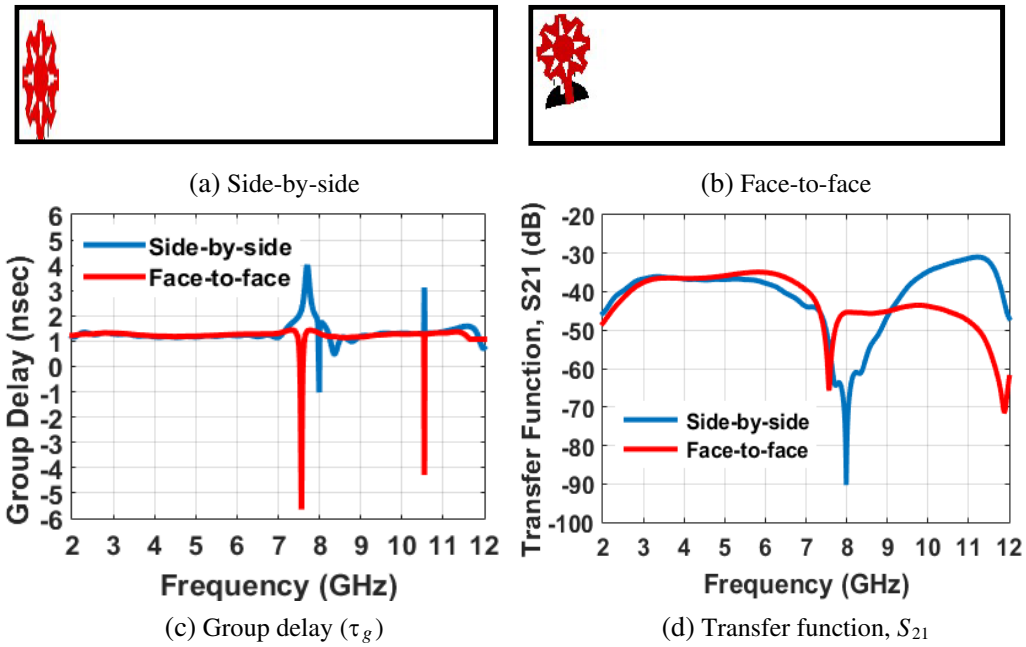

Figure 11. Time domain characteristics of proposed antenna.

4.2. Time Domain Analysis

Figures 11(c) and (d) show the group delay (τ_g) and transfer function (S_{21}) characteristics of the proposed antenna in the time domain for two identical proposed antennas located 30 cm apart in side-

by-side and face-to-face configurations, as depicted in Figures 11(a) and (b), respectively.

The proposed antenna has a flat group delay of about 1.32 ns for side-by-side arrangement and 1.21 ns for face-to-face arrangement, except for notched bands, where the group delay variations are less than 1 ns, which shows that the proposed ESA has strong linear transmission characteristics [16]. The group delay rapidly changes to −5.64 ns and −4.28 ns in face-to-face and 4.03 ns and 3.02 ns in side-by-side configuration for down/uplink of X-band notched frequencies at 7.56 GHz and 10.54 GHz. As shown in Figure 11(d), the isolation (S_{21}) between two proposed antennas is found to be less than −35 dB in both configurations.

The performance comparison of proposed antenna with reported antennas is depicted in Table 2. The following is the major advantages of proposed antenna over reported antennas [17–21],

(i) The proposed antenna size is compact ($24 \times 28\,\text{mm}^2$).
(ii) Wider impedance bandwidth of 2.9–11.75 GHz.
(iii) Being capable of rejecting two notched bands by utilizing a single parasitic.
(iv) The peak radiation efficiency of 92.3%.
(v) The peak gain fluctuation in operating bandwidth is in between 1.4–5.7 dBi.

Table 2. Comparison between proposed and literature antennas.

Ref.	Dimension (mm^2)	Electrical Size	Area (mm^2)	Bandwidth (GHz)	Notched bands	Notch Centre frequency (GHz)	No. of Notched Elements	Efficiency (%)	Gain (dBi)
[17]	30×30	$0.31\lambda_0 \times 0.31\lambda_0$	900	3.1–15	3.3–3.7, 5.15–5.8	6, 6.53	2	NR	2.3–5
[18]	42×45	$0.40\lambda_0 \times 0.43\lambda_0$	1890	2.9–16	5–6.1, 7–8.4	5.5, 7.5	2	NR	NR
[19]	25×35	$0.21\lambda_0 \times 0.29\lambda_0$	875	2.5–13	3.3–3.9, 4.7–5.85	3.6, 5.35	2	NR	2.3–5.5
[20]	30×30	$0.25\lambda_0 \times 0.25\lambda_0$	900	2.45–12	5.12–6, 7.1–7.63	5.4, 7.8	2	90	1.21–4.9
[21]	30×30	$0.34\lambda_0 \times 0.34\lambda_0$	900	3.4–12	3.3–3.9, 5.2–5.9	3.5, 5.5	2	85	2.1–4.9
Prop.	$\mathbf{24 \times 28}$	$\mathbf{0.23\lambda_0 \times 0.27\lambda_0}$	**672**	**2.9–11.75**	**6.8–8.0, 9.7–11.3**	**7.5, 10.5**	**1**	**92.3**	**1.4–5.7**

NR: Not Reported, λ_0: Wavelength at lower frequency.

5. CONCLUSION

A novel circularly slotted UWB antenna with dual band notched features that utilises a single parasitic element has been developed. To produce a UWB bandwidth of 2.9–11.75 GHz, the proposed antenna includes a novel slotted circular patch and a novel elliptically slotted DGS. Two rejected bands for downlink of X-band (6.8–8 GHz) and uplink of X-band (9.7–11.3 GHz) applications are obtained by etching an inverted U-shaped parasitic element on top of the DGS. The proposed antenna has a gain fluctuation of 1.4–5.7 dBi and a peak radiation efficiency of 92.3% in the frequency domain, as well as a flat group delay less than 1 ns and isolation less than −35 dB in both side-by-side and face-to-face configurations, making it a suitable candidate for down and uplink X-band notched UWB applications.

REFERENCES

1. Koteswara Rao Devana, V. N. and A. Maheswara Rao, "A compact flower slotted dual band notched ultrawideband antenna integrated with Ku band for ultrawideband, medical, direct broadcast service, and fixed satellite service applications," *Microwave and Optical Technology Letters*, Vol. 63, No. 2, 556–563, 2021.
2. Wu, Q., R. Jin, and J. Geng, "Pulse preserving capabilities of printed circular disk monopole antennas with different grounds for the specified input signal forms," *IEEE Transactions on Antennas and Propagation*, Vol. 55, No. 10, 2866–2873, 2007.
3. Koteswara Rao Devana, V. N., B. S. L. Mounika, B. Yamini, G. Anitha, and G. Bala Sai Tarun, "Novel UWB monopole antenna with band notched characteristics," *International Journal of Signal Processing, Image Processing and Pattern Recognition*, Vol. 9, No. 5, 291–296, 2016.
4. Naser-Moghadasi, M., A. Danideh, R. Sadeghifakhr, and M. Reza-Azadi, "CPW-fed ultra wideband slot antenna with arc-shaped stub," *IET Microwaves, Antennas & Propagation*, Vol. 3, No. 4, 68–686, 2009.
5. Koteswara Rao Devana, V. N. and A. Maheswara Rao, "Dual band rejection UWB antenna using slot and a novel modified Ψ-shaped parasitic," *2020 7th International Conference on Smart Structures and Systems (ICSSS)*, 1–4, 2020, DOI: 10.1109/ICSSS49621.2020.9202357.
6. Koteswara Rao Devana, V. N., "A novel UWB monopole antenna with defected ground structure," *International Journal of Signal Processing, Image Processing and Pattern Recognition*, Vol. 10, No. 1, 89–98, 2017.
7. Koteswara Rao Devana, V. N. and A. Maheswara Rao, "A novel fan shaped UWB antenna with band notch for WLAN using a simple parasitic slit," *International Journal of Electronics Letters*, Vol. 7, No. 3, 352–366, 2019.
8. Jiang, W. and W. Che, "A novel UWB antenna with dual notched bands for WiMAX and WLAN application," *IEEE Antennas and Wireless Propagation Letters*, Vol. 11, 293–296, 2012.
9. Koteswara Rao Devana, V. N. and A. Maheswara Rao, "Design and parametric analysis of beveled UWB triple band rejection antenna," *Progress In Electromagnetics Research M*, Vol. 84, 95–106, 2019.
10. Koteswara Rao Devana, V. N. and A. Maheswara Rao, "Compact UWB monopole antenna with quadruple band notched characteristics," *International Journal of Electronics*, Vol. 107, No. 2, 175–196, 2020.
11. Rahman, M. and J.-D. Park, "The smallest form factor UWB antenna with quintuple rejection bands for iot applications utilizing RSRR and RCSRR," *Sensors*, Vol. 18, No. 3, 1–16, 2018.
12. Koteswara Rao Devana, V. N. and A. Maheswara Rao, "A novel dual band notched MIMO UWB antenna," *Progress In Electromagnetics Research Letters*, Vol. 93, 65–71, 2020.
13. Koteswara Rao Devana, V. N. and A. Maheswara Rao, "A novel compact fractal UWB antenna with dual band notched characteristics," *Analog Integrated Circuits and Signal Processing*, Vol. 110, 349–360, 2022.
14. Koteswara Rao Devana, V. N. and A. Maheswara Rao, "A novel compact tri band notched UWB monopole antenna," *Progress In Electromagnetics Research M*, Vol. 91, 123–134, 2020.
15. Koteswara Rao Devana, V. N. and A. Maheswara Rao, "Design and analysis of dual band notched UWB antenna using a slot in feed and asymmetrical parasitic," *IETE Journal of Research*, 2020, DOI: 10.1080/03772063.2020.1816226.
16. Koteswara Rao Devana, V. N., E. K. Kumari, K. S. Chakradhar, P. K. Sarma, D. R. Devi, C. M. Kumar, V. D. Raj, and D. R. Prasad, "A novel foot-shaped elliptically embedded patch-ultra wide band antenna with quadruple band notch characteristics verified by characteristic mode analysis," *International Journal of Communication Systems*, Vol. 35, No. 15, e5284, 2022.
17. Din, I. U., S. Ullah, K. Ullah, Y. Fawad, I. Ahmad, S. Ullah, and U. Habib, "Circular monopole ultra-wideband (UWB) antenna with reconfigurable band-notched characteristics," *2020 IEEE 23rd International Multitopic Conference (INMIC)*, 1–6, 2020, DOI: 10.1109/INMIC50486.2020.9318099.

18. Sanyal, R., S. Coomar, D. Chanda (Sarkar), P. S. Bera, and P. P. Sarkar, "Design of UWB monopole antenna with 5.5/7.5 GHz enhanced and controllable dual band rejection characteristics," *2020 IEEE International Conference for Convergence in Engineering*, 325–329, 2020, DOI: 10.1109/ICCE50343.2020.9290693.
19. Li, J. and Y. Su, "Design of reconfigurable monopole antenna with switchable dual band-notches for UWB applications," *Progress In Electromagnetics Research C*, Vol. 96, 97–107, 2019.
20. Sharm, N. and S. S. Bhatia, "Design of printed monopole antenna with band notch characteristics for ultra-wideband applications," *International Journal of RF and Microwave Computer Aided Engineering*, e21894, 2019, DOI: https://doi.org/10.1002/mmce.21894.
21. Ibrahim, A. A., M. A. Abdalla, and A. Boutejdar, "A printed compact band-notched antenna using octagonal radiating patch and meander slot technique for UWB applications," *Progress In Electromagnetics Research M*, Vol. 54, 153–162, 2017.